PHYSICAL REVIEW D **85,** 023529 (2012)

Probing annihilations and decays of low-mass galactic dark matter in IceCube DeepCore array: Track events

Fei-Fan Lee and Guey-Lin Lin

Institute of Physics, National Chiao-Tung University, Hsinchu 30010, Taiwan

(Received 5 July 2011; revised manuscript received 7 December 2011; published 25 January 2012)

The deployment of DeepCore array significantly lowers IceCube's energy threshold to about 10 GeV and enhances the sensitivity of detecting neutrinos from annihilations and decays of light dark matter. To match this experimental development, we calculate the track event rate in DeepCore array due to neutrino flux produced by annihilations and decays of galactic dark matter. We also calculate the background event rate due to the atmospheric neutrino flux for evaluating the sensitivity of DeepCore array to galactic dark matter signatures. Unlike previous approaches, which set the energy threshold for track events at around 50 GeV (this choice avoids the necessity of including the oscillation effect in the estimation of atmospheric background event rate), we have set the energy threshold at 10 GeV to take full advantage of DeepCore array. We compare our calculated sensitivity with those obtained by setting the threshold energy at 50 GeV. We conclude that our proposed threshold energy significantly improves the sensitivity of DeepCore array to the dark matter signature for $m_\chi < 100$ GeV in the annihilation scenario and $m_\chi < 300$ GeV in the decay scenario.

DOI: 10.1103/PhysRevD.85.023529 PACS numbers: 95.35.+d, 14.60.Ef, 14.60.Pq

I. INTRODUCTION

Many astrophysical observations have confirmed the existence of dark matter (DM), which contributes to roughly 23% of the energy density of the Universe. Among many proposed DM candidates, weakly interacting massive particles (WIMPs) [1,2] are popular proposals since they are theoretically well motivated and also capable of producing the correct relic density. WIMPs could annihilate or decay into particles such as electrons, positrons, protons, antiprotons, photons, and neutrinos. It is possible to establish the WIMP signature through detecting these particles [3–15].

Recently, research activities on WIMPs have been boosted in the efforts of explaining the observed anomalous positron excess in the data of PAMELA [8] and positron plus electron excess in the data of FERMI [12]. To account for spectral shapes observed by these experiments, WIMPs must annihilate or decay mostly into leptons in order to avoid the overproduction of antiprotons. This could indicate that DM particles are leptophilic in their annihilations or decays [16,17]. It has been pointed out that the observation of neutrinos can give stringent constraints on the above scenario. Measurements of upward going muons by the Super-Kamiokande observatory place a limit on the galactic muon neutrino flux, which in turn rules out the possibility of WIMP annihilations to $\tau^+\tau^-$ as a source of $e^\pm$ anomalies [18–20]. Furthermore, one expects that the possibilities of WIMP annihilations into $\mu^\pm$, and WIMP decays into $\mu^\pm$ and $\tau^\pm$, will all be stringently constrained [21–23] (see also discussions in Ref. [24]) by the data from IceCube detector augmented with DeepCore array.

The DeepCore array [25,26] is located in the deep center region of IceCube detector. This array consists of six densely instrumented strings plus seven nearest standard IceCube strings. The installation of DeepCore array significantly improves the rejection of downward going atmospheric muons in IceCube and lowers the threshold energy for detecting muon track or cascade events to about 5 GeV. As summarized in Ref. [26], the low detection threshold of DeepCore array is achieved by three improvements over the IceCube detector. First, the photo-sensors in the DeepCore are more densely instrumented than those of IceCube, as just mentioned. Second, the ice surrounding the DeepCore array is on average twice as clear as the average ice above 2000 m [27]. Such a property is useful for reconstructing lower-energy neutrino events. Finally, the DeepCore array uses new type of phototube which has a higher quantum efficiency.

It is clear that DeepCore array improves the sensitivity as well as enlarges the energy window for observing neutrinos from DM annihilations or decays in the galactic halo. Previous analyses on the detection of these neutrinos in the DeepCore [23,28] have set the threshold energy at 40–50 GeV for both track and cascade events. For neutrino events with energies higher than 50 GeV, the estimation of atmospheric background event rate is straightforward since oscillation effects can be neglected. However, to take the full advantage of DeepCore array, it is desirable to estimate the track and shower event rates due to atmospheric neutrinos in the energy range $10\ \text{GeV} \leq E_\nu \leq 50\ \text{GeV}$. In this energy range, the oscillations of atmospheric neutrinos cannot be neglected. In this article, we take into account this oscillation effect and calculate the track event rate with a threshold energy $E_\mu^{\text{th}} = 10$ GeV due to atmospheric

muon neutrinos from all zenith angles. Given such a background event rate, we then evaluate the sensitivities of DeepCore array to the neutrino flux arising from DM annihilations and decays in the galactic halo. In the subsequent paper, we shall analyze the corresponding sensitivities associated with cascade events.

This paper will focus on neutrino signature induced by low-mass DM. Hence our interested DM mass range is far below TeV level implied by PAMELA and FERMI data. Therefore, we shall consider neutrino flux induced by DM annihilations/decays into both leptons and hadrons. Specifically, we consider the channels $\chi\chi \to b\bar{b}, \tau^+\tau^-$, and $\mu^+\mu^-$ for annihilations, and the channels $\chi \to b\bar{b}, \tau^+\tau^-$ and $\mu^+\mu^-$ for decays. Since we are only interested in low-mass dark matter, we have neglected neutrino fluxes generated through DM annihilations or decays into $t\bar{t}$, W^+W^-, and ZZ final states. We also neglect neutrino fluxes arising from light meson decays, as the annihilation cross section for $\chi\chi \to q\bar{q}$ is likely to be suppressed by m_q^2 [2]. We shall compare the constraints on DM annihilation cross section and DM decay time for different values of threshold energy $E_\mu^{\rm th}$. For such a comparison, we employ the modes $\chi\chi \to \mu^+\mu^-$ and $\chi \to \mu^+\mu^-$ for illustrations.

This paper is organized as follows. In Sec. II, we outline the calculation of muon neutrino flux from WIMP annihilations and decays in the galactic halo. In Sec. III, we calculate the atmospheric muon neutrino flux from all zenith angles with $E_\nu \geq 10$ GeV. The oscillations between ν_μ and ν_τ are taken into account. In Sec. IV, we evaluate the sensitivity of DeepCore array to neutrino flux arising from WIMP annihilations or decays in the galactic halo. We compare our results with those obtained by setting $E_\mu^{\rm th} = 50$ GeV. We summarize in Sec. V.

II. NEUTRINO FLUX FROM ANNIHILATIONS AND DECAYS OF DARK MATTER IN THE GALACTIC HALO

The differential neutrino flux from the galactic dark matter halo for neutrino flavor i can be written as [20]

$$\frac{d\Phi_{\nu_i}}{dE_{\nu_i}} = \frac{\Delta\Omega}{4\pi}\frac{\langle\sigma v\rangle}{2m_\chi^2}\left(\sum_F B_F \frac{dN_{\nu_i}^F}{dE}\right) R_\odot \rho_\odot^2 \times J_2(\Delta\Omega) \quad (1)$$

for the case of annihilating DM, and

$$\frac{d\Phi_{\nu_i}}{dE_{\nu_i}} = \frac{\Delta\Omega}{4\pi}\frac{1}{m_\chi \tau_\chi}\left(\sum_F B_F \frac{dN_{\nu_i}^F}{dE}\right) R_\odot \rho_\odot \times J_1(\Delta\Omega) \quad (2)$$

for the case of decaying DM, where $R_\odot = 8.5$ kpc is the distance from the galactic center (GC) to the solar system, $\rho_\odot = 0.3$ GeV/cm^3 is the DM density in the solar neighborhood, m_χ is the DM mass, τ_χ is the DM decay time, and $dN_{\nu_i}^F/dE$ is the neutrino spectrum per annihilation or decay for a given annihilation or decay channel F with a corresponding branching fraction B_F. The neutrino spectra $dN_{\nu_i}^F/dE$ for different channels are summarized in Refs. [28,29]. The quantity $\langle\sigma v\rangle$ is the thermally averaged annihilation cross section, which can be written as

$$\langle\sigma v\rangle = B\langle\sigma v\rangle_0, \quad (3)$$

with a boost factor B [30,31]. We set $\langle\sigma v\rangle_0 = 3 \times 10^{-26}$ cm^3 s^{-1}, which is the typical annihilation cross section for the present dark matter abundance under the standard thermal relic scenario [1]. We treat the boost factor B as a phenomenological parameter. The dimensionless quantity $J_n(\Delta\Omega)$ is the DM distribution integrated over the line-of-sight (l.o.s.) and averaged over a solid angle $\Delta\Omega = 2\pi(1 - \cos\psi_{\rm max})$, i.e.,

$$J_n(\Delta\Omega) = \frac{1}{\Delta\Omega}\int_{\Delta\Omega} d\Omega \int_{\rm l.o.s.} \frac{dl}{R_\odot}\left(\frac{\rho(r(l,\psi))}{\rho_\odot}\right)^n, \quad (4)$$

where ρ is the DM density at a specific location described by the coordinate (l, ψ), with l the distance from the Earth to DM and ψ the direction of DM viewed from the Earth with $\psi = 0$ corresponding to the direction of GC. The distance $r \equiv \sqrt{R_\odot^2 + l^2 - 2R_\odot l\cos\psi}$ is the distance from GC to DM. The upper limit of the integration, $l_{\rm max} \equiv R_\odot\cos\psi + \sqrt{R_s^2 - R_\odot^2\sin^2\psi}$, depends on R_s, the adopted size of the galactic halo. In this analysis, we take $R_s = 20$ kpc and use the Navarro-Frenk-White (NFW) DM density profile [32]

$$\rho(r) = \rho_s\left(\frac{R_s}{r}\right)\left(\frac{R_s}{R_s + r}\right)^2, \quad (5)$$

with $\rho_s = 0.26$ GeV cm^{-3} such that $\rho_\odot = 0.3$ GeV cm^{-3}.

Neutrinos are significantly mixed through oscillations when they travel a vast distance across the galaxy. We determine neutrino flavor oscillation probabilities in the tribimaximal limit [33] of neutrino mixing angles, i.e., $\sin^2\theta_{23} = 1/2$, $\sin^2\theta_{12} = 1/3$, and $\sin^2\theta_{13} = 0$. The neutrino fluxes on Earth are related to those at the source through [34–36]

$$\Phi_{\nu_e} = \tfrac{5}{9}\Phi_{\nu_e}^0 + \tfrac{2}{9}\Phi_{\nu_\mu}^0 + \tfrac{2}{9}\Phi_{\nu_\tau}^0, \quad (6)$$

and

$$\Phi_{\nu_\mu} = \Phi_{\nu_\tau} = \tfrac{2}{9}\Phi_{\nu_e}^0 + \tfrac{7}{18}\Phi_{\nu_\mu}^0 + \tfrac{7}{18}\Phi_{\nu_\tau}^0, \quad (7)$$

where $\Phi_{\nu_i}^0$ is the neutrino flux of flavor i at the astrophysical source. It is understood that the recent T2K [37] and Double Chooz [38] experiments have indicated a nonzero value for θ_{13}. Taking the T2K best-fit value $\sin^2 2\theta_{13} = 0.11$ at the CP phase $\delta = 0$ for the normal mass hierarchy, we have

$$\begin{aligned}
\Phi_{\nu_e} &= 0.53\Phi_{\nu_e}^0 + 0.26\Phi_{\nu_\mu}^0 + 0.21\Phi_{\nu_\tau}^0,\\
\Phi_{\nu_\mu} &= 0.26\Phi_{\nu_e}^0 + 0.37\Phi_{\nu_\mu}^0 + 0.37\Phi_{\nu_\tau}^0,\\
\Phi_{\nu_\tau} &= 0.21\Phi_{\nu_e}^0 + 0.37\Phi_{\nu_\mu}^0 + 0.42\Phi_{\nu_\tau}^0.
\end{aligned} \quad (8)$$

To proceed our discussions, let us first take the neutrinos at the source to be those generated by B meson decays following the $\chi\chi \to b\bar{b}$ annihilation. In this special case, $\Phi^0_{\nu_e} = \Phi^0_{\nu_\mu} = \Phi^0_{\nu_\tau}$ at the source, and consequently the relation $\Phi_{\nu_e} = \Phi_{\nu_\mu} = \Phi_{\nu_\tau}$ always holds due to the probability conservation, irrespective of the form of oscillation probability matrix. Let us now consider neutrinos produced at the source by muon decays following the $\chi\chi \to \mu^+\mu^-$ annihilation. In this case, one has $\Phi^0_{\nu_e} = \Phi^0_{\nu_\mu}$ and $\Phi^0_{\nu_\tau} = 0$. Taking $\Phi^0_{\nu_e} = \Phi^0_{\nu_\mu} \equiv \Phi^0$, one obtains $\Phi_{\nu_e} = 0.78\Phi^0$ and $\Phi_{\nu_\mu} = \Phi_{\nu_\tau} = 0.61\Phi^0$ for tribimaximal values of neutrino mixing parameters. On the other hand, with the T2K best-fit θ_{13} value, one arrives at $\Phi_{\nu_e} = 0.79\Phi^0$, $\Phi_{\nu_\mu} = 0.63\Phi^0$ and $\Phi_{\nu_\tau} = 0.58\Phi^0$ for the normal mass hierarchy. Clearly Φ_{ν_e} is almost unaffected while $\Phi_{\nu_\mu}/\Phi_{\nu_\tau} - 1 = 9\%$. For the inverted mass hierarchy, one obtains the same ν_e flux while $\Phi_{\nu_\mu}/\Phi_{\nu_\tau} - 1 = 12\%$. Hence T2K result implies an $O(10\%)$ difference between the arrival ν_μ and ν_τ fluxes for neutrinos produced by $\chi\chi \to \mu^+\mu^-$ annihilations. Since this effect is not large and it is not possible to identify ν_τ in our interested energy range, we shall still apply Eqs. (6) and (7) for determining the arrival neutrino fluxes.

III. ATMOSPHERIC NEUTRINO FLUXES

Knowing atmospheric neutrino background is important for evaluating the sensitivity of DeepCore array to neutrino flux from DM annihilations or decays. We begin by computing the flux of intrinsic atmospheric muon neutrinos arising from pion and kaon decays, following the approaches in Refs. [39,40]. The ν_μ flux arising from π decays can be written as

$$\begin{aligned}\frac{\mathrm{d}^2 N^\pi_{\nu_\mu}(E,\xi,X)}{\mathrm{d}E\mathrm{d}X} &= \int_E^\infty \mathrm{d}E_N \int_E^{E_N} \mathrm{d}E_\pi \frac{\Theta(E_\pi - \frac{E}{1-\gamma_\pi})}{d_\pi E_\pi (1-\gamma_\pi)} \\ &\times \int_0^X \frac{\mathrm{d}X'}{\lambda_N} P_\pi(E_\pi, X, X') \frac{1}{E_\pi} F_{N\pi}(E_\pi, E_N) \\ &\times \exp\left(-\frac{X'}{\Lambda_N}\right)\phi_N(E_N), \end{aligned} \tag{9}$$

where E is the neutrino energy, X is the slant depth in units of g/cm^2, ξ is the zenith angle in the direction of incident cosmic-ray nucleons, $r_\pi = m_\mu^2/m_\pi^2$, d_π is the pion decay length in units of g/cm^2, λ_N is the nucleon interaction length, and Λ_N is the corresponding nucleon attenuation length. The function $P_\pi(E_\pi, X, X')$ is the probability that a charged pion produced at the slant depth X' survives to the depth X ($> X'$), which is given by [41]

$$\begin{aligned} P_\pi(E_\pi, X, X') &= \exp\left(-\frac{X - X'}{\Lambda_\pi}\right) \\ &\cdot \exp\left(-\frac{m_\pi c}{E_\pi \tau_\pi}\int_{X'}^{X} \frac{\mathrm{d}T}{\rho(T)}\right), \end{aligned} \tag{10}$$

where $\Lambda_\pi = 160$ g/cm^2 is the pion attenuation length, τ_π is the pion lifetime at its rest frame, while $\rho(T)$ is the atmosphere mass density at the slant depth T. Finally, $F_{N\pi}(E_\pi, E_N)$ is the normalized inclusive cross section for $N + \text{air} \to \pi^\pm + Y$, which is given by [39]

$$\begin{aligned} F_{N\pi}(E_\pi, E_N) &\equiv \frac{E_\pi}{\sigma_N}\frac{\mathrm{d}\sigma(E_\pi, E_N)}{\mathrm{d}E_\pi} \\ &= c_+(1-x)^{p_+} + c_-(1-x)^{p_-}, \end{aligned} \tag{11}$$

with $x = E_\pi/E_N$, $c_+ = 0.92$, $c_- = 0.81$, $p_+ = 4.1$, and $p_- = 4.8$.

The primary cosmic-ray spectrum $\phi_N(E_N)$ in Eq. (9) includes contributions from cosmic ray protons and those from heavier nuclei. We have $\phi_N(E_N) = \sum_A A\phi_A(E_N)$ with A as the atomic number of each nucleus. The spectrum of each cosmic-ray component is parametrized by [42,43]

$$\phi_A(E_N) = K \times (E_N + b\exp[-c\sqrt{E_N}])^{-\alpha}, \tag{12}$$

in units of m^{-2} s^{-1} sr^{-1} GeV^{-1}. The fitting parameters α, K, b, c depend on the type of nucleus. They are tabulated in Table I [43]. The kaon contribution to the atmospheric ν_μ flux has the same form as Eq. (9) with an inclusion of the branching ratio $B(K \to \mu\nu) = 0.635$ and appropriate replacements in kinematic factors and the normalized inclusive cross section. In particular, $F_{NK}(E_K, E_N)$ can be parametrized as Eq. (11) with $c_+ = 0.037$, $c_- = 0.045$, $p_+ = 0.87$, and $p_- = 3.5$.

Since our interested energy range is as low as 10 GeV, the three-body muon decay contribution to the atmospheric ν_μ flux is not negligible, particularly in the near horizontal direction. To obtain this part of contribution, we first compute the atmospheric muon flux from pion and kaon decays. The muon flux induced by pion decays is given by [39,40]

TABLE I. Parameters for all five components in the fit of Eq. (12).

Parameter/component	α	K	b	c
Hydrogen ($A = 1$) ($\leq 10^2$ GeV)	2.74	14 900	2.15	0.21
Hydrogen ($A = 1$) ($>10^2$ GeV)	2.71	14 900	2.15	0.21
He ($A = 4$)	2.64	600	1.25	0.14
CNO ($A = 14$)	2.60	33.2	0.97	0.01
MgSi ($A = 25$)	2.79	34.2	2.14	0.01
Iron ($A = 56$)	2.68	4.45	3.07	0.41

$$\frac{dN_\mu^\pi(E,\xi,X)}{dE} = \int_{E'}^{\infty} dE_N \int_{E'}^{E_N} dE_\pi \int_0^X dX'' P_\mu(E,X,X'') \times \frac{\Theta(E_\pi - E')\Theta(\frac{E'}{r_\pi} - E_\pi)}{d_\pi E_\pi (1-r_\pi)} \times \int_0^{X''} \frac{dX'}{\lambda_N} P_\pi(E_\pi, X'', X') \times \frac{1}{E_\pi} F_{N\pi}(E_\pi, E_N) \exp\left(-\frac{X'}{\Lambda_N}\right) \phi_N(E_N), \quad (13)$$

where E' and E are muon energies at slant depths X'' and X, respectively, while $P_\mu(E,X,X'')$ is the muon survival probability. The muon flux induced by kaon decays can be calculated in a similar way. Since $\mu^-(\mu^+)$ produced by $\pi^-(\pi^+)$ decays are polarized, we classify muon flux into four different components such as $dN^{\pi^+}_{\mu_R^+}/dE$, $dN^{\pi^-}_{\mu_R^-}/dE$, $dN^{\pi^+}_{\mu_L^+}/dE$, and $dN^{\pi^-}_{\mu_L^-}/dE$. We also calculate additional four components of the muon flux arising from the kaon decays. Hence the ν_μ flux arising from muon decays can be written as [40,41]

$$\frac{d^2N^{\mu^\pm}_{\nu_\mu}(E,\xi,X)}{dE dX} = \sum_{s=L,R} \int_E^\infty dE_\mu \frac{F_{\mu_s^\pm \to \nu_\mu}(E/E_\mu)}{d_\mu(E_\mu,X)E_\mu} \times \frac{dN_{\mu_s^\pm}(E_\mu,\xi,X)}{dE_\mu}, \quad (14)$$

where $d_\mu(E_\mu,X)$ is the muon decay length in units of g/cm^2 at the slant depth X, and $F_{\mu_s^\pm \to \nu_\mu}(E/E_\mu)$ is the normalized decay spectrum of $\mu_s^\pm \to \nu_\mu$. Summing the two-body and three-body decay contributions, we obtain the total intrinsic atmospheric muon neutrino flux. In Fig. 1, we show the comparison of angle-averaged atmospheric muon neutrino flux obtained by our calculation and that obtained by Honda *et al.* [44]. At $E_\nu = 10$ GeV, two calculations only differ by 3%. At $E_\nu = 100$ GeV, the difference is 10%. We also show in the same figure the atmospheric muon neutrino flux measured by AMANDA-II detector [45]. It is seen that both calculations agree well with AMANDA results.

To completely determine the atmospheric muon neutrino flux, one also needs to calculate the intrinsic atmospheric tau neutrino flux, although this part of contribution is rather small. The intrinsic atmospheric ν_τ flux arises from D_s decays. This flux can be obtained by solving cascade equations [40,46]. We obtain

$$\frac{d^2N_{\nu_\tau}(E,X)}{dE dX} = \frac{Z_{ND_s} Z_{D_s\nu_\tau}}{1-Z_{NN}} \cdot \frac{\exp(-X/\Lambda_N)\phi_N(E_N)}{\Lambda_N}, \quad (15)$$

where $Z_{NN} \equiv 1 - \lambda_N/\Lambda_N$ and Z_{ND_s} is a special case of the generic expression

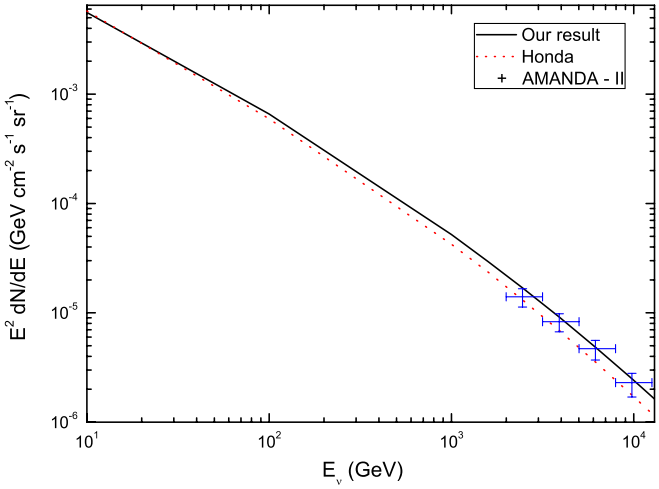

FIG. 1 (color online). The comparison of angle-averaged atmospheric muon neutrino ($\nu_\mu + \bar{\nu}_\mu$) flux obtained by our calculation and that obtained by Honda *et al.* [44]. Angle-averaged $\nu_\mu + \bar{\nu}_\mu$ flux from AMANDA-II measurements [45] is also shown.

$$Z_{ij}(E_j) \equiv \int_{E_j}^\infty dE_i \frac{\phi_i(E_i)}{\phi_i(E_j)} \frac{\lambda_i(E_j)}{\lambda_i(E_i)} \frac{dn_{iA\to jY}(E_i,E_j)}{dE_j}, \quad (16)$$

with $dn_{iA\to jY}(E_i,E_j) \equiv d\sigma_{iA\to jY}(E_i,E_j)/\sigma_{iA}(E_i)$ and λ_i the interaction length of particle i in units of g/cm^2. The decay moment $Z_{D_s\nu_\tau}$ is given by

$$Z_{D_s\nu_\tau}(E_{\nu_\tau}) \equiv \int_{E_{\nu_\tau}}^\infty dE_{D_s} \frac{\phi_{D_s}(E_{D_s})}{\phi_{D_s}(E_{\nu_\tau})} \times \frac{d_{D_s}(E_{\nu_\tau})}{d_{D_s}(E_{D_s})} F_{D_s\to\nu_\tau}(E_{\nu_\tau}/E_{D_s}), \quad (17)$$

where d_{D_s} is the decay length of D_s and $F_{D_s\to\nu_\tau}(E_{\nu_\tau}/E_{D_s})$ is the normalized decay distribution. In this work, we employ the next-to-leading order perturbative QCD [47] with CTEQ6 parton distribution functions to calculate the differential cross section of $NA \to c\bar{c}$ and determine Z_{ND_s}.

Finally, the atmospheric ν_μ flux taking into account the neutrino oscillation effect is given by

$$\frac{d\bar{N}_{\nu_\mu}(E,\xi)}{dE} = \int dX \left[\frac{d^2N_{\nu_\tau}}{dE dX} \cdot P_{\nu_\tau\to\nu_\mu} + \frac{d^2N_{\nu_\mu}}{dE dX} \cdot (1 - P_{\nu_\mu\to\nu_\tau})\right], \quad (18)$$

where $P_{\nu_\mu\to\nu_\tau}(E,L(X,\xi)) = P_{\nu_\tau\to\nu_\mu}(E,L(X,\xi)) \equiv \sin^2 2\theta_{23}\sin^2(1.27\Delta m^2_{31}L/E)$ is the $\nu_\mu \to \nu_\tau$ oscillation probability and $L(X,\xi)$ is the linear distance from the neutrino production point to the position of IceCube DeepCore array. The unit of Δm^2_{31} is eV^2 while L and E are in units of km and GeV, respectively. The best-fit values for oscillation parameters obtained from a recent analysis [48] are $\Delta m^2_{31} = 2.47 \cdot 10^{-3}$ eV^2 and $\sin^2 2\theta_{23} = 1$, respectively.

IV. RESULTS

In IceCube DeepCore, the event rate for contained muons is given by

$$\Gamma_\mu = \int_{E_\mu^{\rm th}}^{E_{\rm max}} dE_\mu \int_{E_\mu}^{E_{\rm max}} dE_{\nu_\mu} N_A \rho_{\rm ice} V_{\rm tr} \frac{d\Phi_{\nu_\mu}}{dE_{\nu_\mu}} \cdot \frac{d\sigma_{\nu N}^{\rm CC}(E_{\nu_\mu}, E_\mu)}{dE_\mu} + (\nu \to \bar{\nu}), \quad (19)$$

where $\rho_{\rm ice} = 0.9\ {\rm g\,cm^{-3}}$ is the density of ice, $N_A = 6.022 \times 10^{23}\ {\rm g^{-1}}$ is the Avogadro number, $V_{\rm tr} \approx 0.04\ {\rm km^3}$ is the effective volume of IceCube DeepCore array for muon track events [25], $d\Phi_{\nu_\mu}/dE_{\nu_\mu}$ is the muon neutrino flux arrived at IceCube, $E_{\rm max}$ is taken as m_χ for annihilation and $m_\chi/2$ for decay, and $E_\mu^{\rm th}$ is the threshold energy for muon track events. In this work, we use differential cross sections $d\sigma_{\nu N}^{\rm CC}(E_{\nu_\mu}, E_\mu)/dE_\mu$ given by Ref. [49] with CTEQ6 parton distribution functions. We also set $E_\mu^{\rm th} = 10$ GeV.

As stated before, we consider neutrino fluxes generated by the annihilation channels $\chi\chi \to b\bar{b}, \tau^+\tau^-$ and $\mu^+\mu^-$, and the decay channels $\chi \to b\bar{b}, \tau^+\tau^-$ and $\mu^+\mu^-$. Given the atmospheric neutrino background, we present in Fig. 2 the required DM annihilation cross section as a function of m_χ for threshold energy $E_\mu^{\rm th} = 10$ GeV and a cone half-angle $\psi_{\rm max} = 1^\circ$ such that the neutrino signature from DM annihilations can be detected at the 2σ significance in five years. Nondetection of such a signature would then exclude the parameter region above the curve at the 2σ level. We have presented results corresponding to different annihilation channels. One can see that the required annihilation cross section for 2σ detection significance is smallest for the $\chi\chi \to \mu^+\mu^-$ channel and largest for the channel $\chi\chi \to b\bar{b}$. We also present the 3σ constraint on $\chi\chi \to \tau^+\tau^-$ annihilation cross section obtained from Super-Kamiokande data of upward going muons [18], which has been used to rule out WIMP annihilations into $\tau^+\tau^-$ as a possible source of previously mentioned $e^\pm$ anomalies [18–20]. Such a constraint can be compared with the expected 2σ constraint on the same annihilation channel from the DeepCore detector.

Constraints on DM annihilation cross section were also obtained from gamma ray observations and cosmology. The H.E.S.S. telescope performed a search for the very high-energy (≥ 100 GeV) γ-ray signal from DM annihilations over a circular region of radius 1° centered at the GC [50]. With DM particles assumed to annihilate into $q\bar{q}$ pairs, the limit on DM annihilation cross section as a function of m_χ for NFW DM density profile is derived in Ref. [50]. We present this constraint in Fig. 2 as well. For $m_\chi > 300$ GeV, the parameter space with $B > 100$ (i.e., $\langle\sigma v\rangle > 3 \times 10^{-24}\ {\rm m^3\,s^{-1}}$) in Fig. 2 could be excluded by the H.E.S.S. data. However, the H.E.S.S. constraint on $\chi\chi \to q\bar{q}$ becomes much weaker for $m_\chi < 300$ GeV. We point out that this constraint is obtained with NFW profile normalized at $\rho_\odot = 0.39\ {\rm GeV\ cm^{-3}}$. The H.E.S.S. constraint would be slightly less stringent if our adopted normalization $\rho_\odot = 0.3\ {\rm GeV\ cm^{-3}}$ is used.

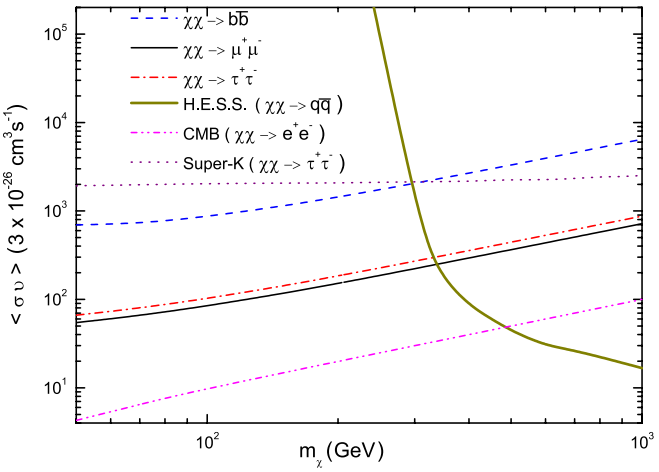

FIG. 2 (color online). The dashed line, thin solid line, and dot-dashed lines are the expected constraints on DM annihilation cross section by the DeepCore detector for $\chi\chi \to b\bar{b}$, $\chi\chi \to \mu^+\mu^-$, and $\chi\chi \to \tau^+\tau^-$ channels, respectively. The thick solid line is the H.E.S.S constraint on the annihilation cross section of DM into the light quark pair $\chi\chi \to q\bar{q}$ [50]. The dot-dot-dashed line is the constraint on $\chi\chi \to e^+e^-$ annihilation cross section from the analysis of cosmic microwave background data [51]. The dotted line is the 3σ constraint on the annihilation cross section of $\chi\chi \to \tau^+\tau^-$ from Super-Kamiokande data [18].

Cosmological constraints on DM annihilation cross section can be obtained from the data of big bang nucleosynthesis and cosmic microwave background (CMB). In such an analysis, DM annihilation cross section is assumed to be velocity dependent such that [51]

$$\langle\sigma v\rangle = \frac{\langle\sigma v\rangle_0}{\epsilon + (v/v_0)^n}, \quad (20)$$

where v_0 is DM velocity at the freeze-out temperature, while the values for ϵ and n depend on specific models. For Sommerfeld enhancement [30] of the DM annihilation cross section induced by light-scalar exchange, one has $n = 1$ and $\epsilon \simeq m_\phi/m_\chi$ with m_ϕ the light-scalar mass. The CMB anisotropy can be affected by the energy injection in the recombination epoch due to DM annihilation process such as $\chi\chi \to e^+e^-$ and $\chi\chi \to W^+W^-$. In Fig. 2, we show the upper bound on $\langle\sigma v\rangle$ for $\chi\chi \to e^+e^-$ channel for $n = 1$ and $T_{\rm KD} = 1$ MeV with $T_{\rm KD}$ as the kinetic decoupling temperature. This upper bound is inferred from the upper bound on $\langle\sigma v\rangle_0$ such that the resulting CMB power spectrum remains consistent with observations [51]. The above upper bound on $\langle\sigma v\rangle_0$ is shown to be sensitive to the parameter ϵ while the corresponding bound on $\langle\sigma v\rangle$ is insensitive to it. It will be interesting to

convert the above bound on $\langle\sigma(\chi\chi \to e^+e^-)v\rangle$ into the one on $\langle\sigma(\chi\chi \to \mu^+\mu^-)v\rangle$. However such a conversion is highly model dependent which is beyond the scope of the current work.

Having compared the expected sensitivities of the DeepCore detector with other experimental constraints on various DM annihilation channels, we discuss how the DeepCore constraint on DM annihilation cross section varies with the chosen cone half-angle and threshold energy. We use the channel $\chi\chi \to \mu^+\mu^-$ to illustrate these effects. Figure 3 shows the required DM annihilation cross section $\langle\sigma(\chi\chi \to \mu^+\mu^-)v\rangle$ for a 2σ detection in five years for different cone half-angle $\psi_{\max}$. One can see that the constraint on the DM annihilation cross section gets stronger as $\psi_{\max}$ increases from 1° to 2°. However, the constraint turns weaker as $\psi_{\max}$ increases further. This is due to the factor $J_2(\Delta\Omega)\Delta\Omega$ which depends on the square of DM density [see Eq. (8)]. The constraint curve rises with an increasing $\psi_{\max}$ for $\psi_{\max} > 2°$, since the signal increases slower than the background does for such a $\psi_{\max}$ range. In this figure, we also show the result for a higher threshold energy $E_\mu^{\rm th} = 50$ GeV with a cone half-angle $\psi_{\max} = 10°$ for comparison. This result is taken from Ref. [28] where $\psi_{\max} = 10°$ is identified as the most optimal cone half-angle for constraining DM annihilation cross section at that threshold energy. We note that, for large m_χ, lowering $E_\mu^{\rm th}$ from 50 GeV to 10 GeV results in more enhancement on the event rate of atmospheric background than that of DM annihilation. Hence, the constraint on DM annihilation cross section is weaker by choosing $E_\mu^{\rm th} = 10$ GeV. On the other hand, for small m_χ, lowering $E_\mu^{\rm th}$ enhances more on the event rate of DM annihilations

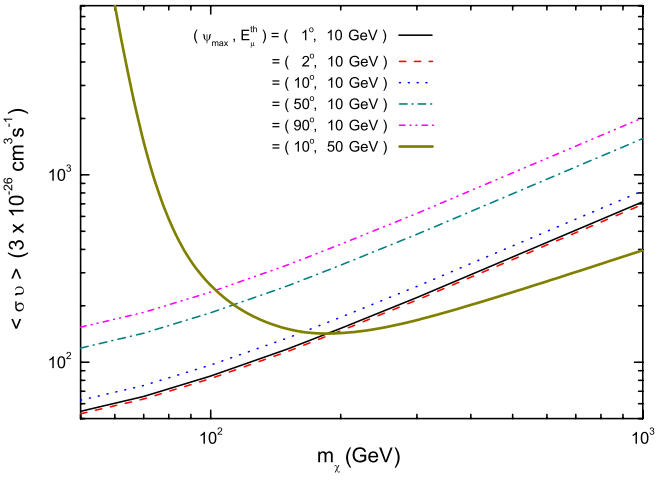

FIG. 3 (color online). The required DM annihilation cross section $(\chi\chi \to \mu^+\mu^-)$ as a function of m_χ such that the neutrino signature from DM annihilations can be detected at the 2σ significance in five years. Results corresponding to different $\psi_{\max}$ are presented. For comparison, we also show the result with $E_\mu^{\rm th} = 50$ GeV and $\psi_{\max} = 10°$ [28].

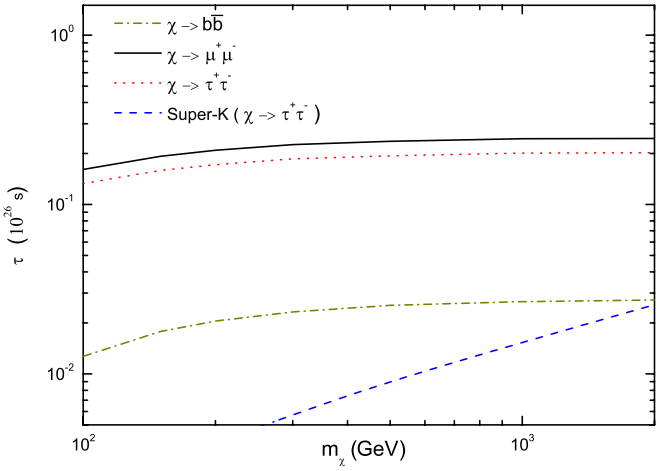

FIG. 4 (color online). The dot-dashed line, solid line, and dotted line are the required DM decay time for a 2σ detection of neutrino signature in five years for $\chi \to b\bar{b}$, $\mu^+\mu^-$ and $\tau^+\tau^-$ channels, respectively. The dashed line is the Super-Kamiokande constraint on $\chi \to \tau^+\tau^-$ [18].

than that of atmospheric background. For $m_\chi < 100$ GeV, one can see that the constraint on DM annihilation cross section with $E_\mu^{\rm th} = 10$ GeV is always stronger than that with $E_\mu^{\rm th} = 50$ GeV. We note that DeepCore constraints on other annihilation channels have similar cone half-angle and threshold energy dependencies.

Besides studying DeepCore constraints on DM annihilation channels, we also present constraints on DM decay time for $\chi \to b\bar{b}$, $\tau^+\tau^-$ and $\mu^+\mu^-$ channels. Figure 4 shows the required DM decay time for a 2σ detection of neutrino signature in five years for each channel. We have taken $E_\mu^{\rm th} = 10$ GeV and $\psi_{\max} = 90°$. Nondetection of such a signature would then exclude the parameter region below the curve at the 2σ level. For comparison, we also show 3σ limit on $\chi \to \tau^+\tau^-$ from Super-Kamiokande data of upward going muons [18]. One can see that the channel $\chi \to \mu^+\mu^-$ requires the smallest decay width to reach the 2σ detection significance in five years of DeepCore data taking.

Finally, we present how the DeepCore constraint on DM decay time varies with the chosen cone half-angle and threshold energy. We use the channel $\chi \to \mu^+\mu^-$ to illustrate these effects. Figure 5 shows the required DM decay time $(\chi \to \mu^+\mu^-)$ as a function of m_χ for different cone half-angle $\psi_{\max}$ such that the neutrino signature from DM decays can be detected at the 2σ significance in five years. For DM decays, the curve rises with increasing $\psi_{\max}$ since the event rate of DM signal increases faster than that of atmospheric background as $\psi_{\max}$ increases. For comparison, we show the required DM decay time for a 2σ detection in five years with $E_\mu^{\rm th} = 50$ GeV and $\psi_{\max} = 50°$. It has been pointed out in Ref. [28] that $\psi_{\max} = 50°$ gives the most stringent constraint on DM decay time for

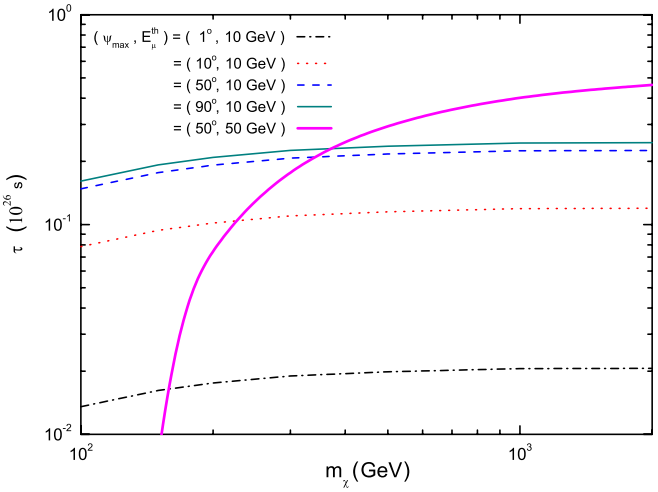

FIG. 5 (color online). The required DM decay time ($\chi \to \mu^+\mu^-$) as a function of m_χ such that the neutrino signature from DM decays can be detected at the 2σ significance in five years. Results corresponding to different $\psi_{\max}$ are presented. For comparison, we also show the result with $E_\mu^{\rm th} = 50$ GeV and $\psi_{\max} = 50°$ [28].

$E_\mu^{\rm th} = 50$ GeV. One can see that the constraint on DM decay time is strengthen by lowering $E_\mu^{\rm th}$ from 50 GeV to 10 GeV for $m_\chi < 300$ GeV.

V. SUMMARY

We have calculated the track event rate in IceCube DeepCore array resulting from muon neutrino flux produced by annihilations and decays of dark matter in the galactic halo. In this calculation, we have employed NFW profile for dark matter mass distribution and consider the channels $\chi\chi \to b\bar{b}, \tau^+\tau^-$, and $\mu^+\mu^-$ for annihilations, and the channels $\chi \to b\bar{b}, \tau^+\tau^-$ and $\mu^+\mu^-$ for decays. We also calculated the track event rate due to atmospheric background. We compare the signal event rate with that of the background for $E_\mu \geq 10$ GeV.

We have presented sensitivities of IceCube DeepCore array to neutrino flux arising from dark matter annihilations and decays. For a given dark matter mass, we evaluated the dark matter annihilation cross section and dark matter decay time such that a 2σ detection significance for the above signatures can be achieved by DeepCore array for a five-year data taking. The DeepCore sensitivities on dark matter annihilation cross section were compared with the constraint obtained from H.E.S.S. gamma ray observations and the constraint derived from the data of CMB power spectrum. Using $\chi\chi \to \mu^+\mu^-$ and $\chi \to \mu^+\mu^-$ as examples, we also presented how DeepCore constraints on dark matter annihilation cross section and dark matter decay time vary with the chosen cone half-angle and threshold energy. We like to point out that our calculated sensitivities based upon $E_\mu^{\rm th} = 10$ GeV are significantly more stringent than those obtained by taking $E_\mu^{\rm th} = 50$ GeV for $m_\chi < 100$ GeV in the annihilation channel and $m_\chi < 300$ GeV in the decay channel.

ACKNOWLEDGMENTS

This work is supported by the National Science Council of Taiwan under Grants No. 099-2811-M-009-055 and No. 99-2112-M-009-005-MY3, and Focus Group on Cosmology and Particle Astrophysics, National Center for Theoretical Sciences, Taiwan.

[1] G. Jungman, M. Kamionkowski, and K. Griest, Phys. Rep. **267**, 195 (1996); L. Bergstrom, Rep. Prog. Phys. **63**, 793 (2000).
[2] G. Bertone, D. Hooper, and J. Silk, Phys. Rep. **405**, 279 (2005).
[3] W. B. Atwood *et al.* (Fermi/LAT Collaboration), Astrophys. J. **697**, 1071 (2009); E. O. Wilhelmi (HESS Collaboration), AIP Conf. Proc. **1112**, 16 (2009); M. Beilicke (VERITAS Collaboration), AIP Conf. Proc. **1112**, 33 (2009); T. Mizukami (CANGAROO-III Collaboration), AIP Conf. Proc. **1085**, 364 (2008); Y. Yukawa (CANGAROO Collaboration), J. Phys.: Conf. Ser. **120**, 062018 (2008); J. Rico *et al.* (MAGIC Collaboration), AIP Conf. Proc. **1112**, 23 (2009).
[4] P. Jean *et al.*, Astron. Astrophys. **407**, L55 (2003); C. Boehm, D. Hooper, J. Silk, M. Casse, and J. Paul, Phys. Rev. Lett. **92**, 101301 (2004).
[5] D. P. Finkbeiner, Astrophys. J. **614**, 186 (2004); G. Dobler and D. P. Finkbeiner, Astrophys. J. **680**, 1222 (2008); M. Bottino, A. J. Banday, and D. Maino, arXiv:0807.1865; D. Hooper, D. P. Finkbeiner, and G. Dobler, Phys. Rev. D **76**, 083012 (2007).
[6] M. Aguilar *et al.* (AMS-01 Collaboration), Phys. Lett. B **646**, 145 (2007); C. Goy (AMS Collaboration), J. Phys. Conf. Ser. **39**, 185 (2006); D. Casadei, arXiv:0609072.
[7] S. W. Barwick *et al.* (HEAT Collaboration), Astrophys. J. **482**, L191 (1997).
[8] O. Adriani *et al.* (PAMELA Collaboration), Nature (London) **458**, 607 (2009); E. Mocchiutti *et al.*, arXiv:0905.2551.
[9] J. Chang *et al.*, Nature (London) **456**, 362 (2008).
[10] S. Torii *et al.* (PPB-BETS Collaboration), arXiv:0809.0760; K. Yoshida *et al.*, Adv. Space Res. **42**, 1670 (2008).
[11] H. E. S. Aharonian, Astron. Astrophys. **508**, 561 (2009).

[12] A. A. Abdo *et al.* (Fermi LAT Collaboration), Phys. Rev. Lett. **102**, 181101 (2009).

[13] J. Braun and D. Hubert (IceCube Collaboration), arXiv:0906.1615; D. Hubert (IceCube Collaboration), Nucl. Phys. B, Proc. Suppl. **173**, 87 (2007).

[14] R. Abbasi *et al.* (IceCube Collaboration), Nucl. Instrum. Methods Phys. Res., Sect. A **601**, 294 (2009); C. Rott (IceCube Collaboration), arXiv:0810.3698.

[15] U. F. Katz (KM3NeT Collaboration), Nucl. Instrum. Methods Phys. Res., Sect. A **602**, 40 (2009).

[16] P. J. Fox and E. Poppitz, Phys. Rev. D **79**, 083528 (2009); R. Harnik and G. D. Kribs, Phys. Rev. D **79**, 095007 (2009); Q. H. Cao, E. Ma, and G. Shaughnessy, Phys. Lett. B **673**, 152 (2009); B. Kyae, J. Cosmol. Astropart. Phys. 07 (2009) 028; X. J. Bi, X. G. He, and Q. Yuan, Phys. Lett. B **678**, 168 (2009); S. Baek and P. Ko, J. Cosmol. Astropart. Phys. 10 (2009) 011; D. J. Phalen, A. Pierce, and N. Weiner, Phys. Rev. D **80**, 063513 (2009); H. S. Goh, L. J. Hall, and P. Kumar, J. High Energy Phys. 05 (2009) 097; A. Ibarra, A. Ringwald, D. Tran, and C. Weniger, J. Cosmol. Astropart. Phys. 08 (2009) 017; Y. Farzan, S. Pascoli, and M. A. Schmidt, J. High Energy Phys. 10 (2010) 111.

[17] V. Barger, Y. Gao, W. Y. Keung, D. Marfatia, and G. Shaughnessy, Phys. Lett. B **678**, 283 (2009).

[18] P. Meade, M. Papucci, A. Strumia, and T. Volansky, Nucl. Phys. **B831**, 178 (2010).

[19] S. Palomares-Ruiz, Phys. Lett. B **665**, 50 (2008).

[20] J. Hisano, M. Kawasaki, K. Kohri, and K. Nakayama, Phys. Rev. D **79**, 043516 (2009).

[21] D. Spolyar, M. R. Buckley, K. Freese, D. Hooper, and H. Murayama, arXiv:0905.4764.

[22] M. R. Buckley, K. Freese, D. Hooper, D. Spolyar, and H. Murayama, Phys. Rev. D **81**, 016006 (2010).

[23] S. K. Mandal, M. R. Buckley, K. Freese, D. Spolyar, and H. Murayama, Phys. Rev. D **81**, 043508 (2010).

[24] L. Covi, M. Grefe, A. Ibarra, and D. Tran, J. Cosmol. Astropart. Phys. 04 (2010) 017.

[25] E. Resconi (IceCube Collaboration), Nucl. Instrum. Methods Phys. Res., Sect. A **602**, 7 (2009).

[26] C. Wiebusch, for the IceCube Collaboration, arXiv:0907.2263.

[27] M. Ackermann *et al.* (IceCube Collaboration), J. Geophys. Res. **111**, D13203 (2006).

[28] A. E. Erkoca, M. H. Reno, and I. Sarcevic, Phys. Rev. D **82**, 113006 (2010).

[29] A. E. Erkoca, G. Gelmini, M. H. Reno, and I. Sarcevic, Phys. Rev. D **81**, 096007 (2010).

[30] A. Sommerfeld, Ann. Phys. (Leipzig) **403**, 257 (1931); J. M. Russell, S. M. West, D. Cumberbatch, and D. Hooper, J. High Energy Phys. 07 (2008) 058; N. Arkani-Hamed, D. P. Finkbeiner, T. R. Slatyer, and N. Weiner, Phys. Rev. D **79**, 015014 (2009); I. Cholis, G. Dobler, D. P. Finkbeiner, L. Goodenough, and N. Weiner, Phys. Rev. D **80**, 123518 (2009); M. Lattanzi and J. Silk, Phys. Rev. D **79**, 083523 (2009); B. Robertson and A. Zentner, Phys. Rev. D **79**, 083525 (2009); M. Kamionkowski, S. M. Koushiappas, and M. Kuhlen, Phys. Rev. D 81, 043532 (2010); S. Hannestad and T. Tram, J. Cosmol. Astropart. Phys. 01 (2011) 016; J. L. Feng, M. Kaplinghat, and H.-B. Yu, Phys. Rev. D **82**, 083525 (2010); C. Arina, F.-X. Josse-Michaux, and N. Sahu, Phys. Lett. B **691**, 219 (2010).

[31] J. Hisano, S. Matsumoto, and M. M. Nojiri, Phys. Rev. Lett. **92**, 031303 (2004); J. M. Russell and S. M. West, Phys. Lett. B **676**, 133 (2009); S. M. Koushiappas and M. Kamionkowski, Phys. Rev. Lett. **103**, 121301 (2009); M. Lindner, A. Merle, and V. Niro, Phys. Rev. D **82**, 123529 (2010); D. Suematsu, T. Toma, and T. Yoshida, Phys. Rev. D **82**, 013012 (2010).

[32] J. F. Navarro, C. S. Frenk, and S. D. M. White, Astrophys. J. **462**, 563 (1996).

[33] P. F. Harrison, D. H. Perkins, and W. G. Scott, Phys. Lett. B **530**, 167 (2002); Phys. Lett. B **535**, 163 (2002); Z. Z. Xing, Phys. Lett. B **533**, 85 (2002); X. G. He and A. Zee, Phys. Lett. B **560**, 87 (2003); see also L. Wolfenstein, Phys. Rev. D **18**, 958 (1978); Y. Yamanaka, H. Sugawara, and S. Pakvasa, Phys. Rev. D **25**, 1895 (1982); **29**, 2135(E) (1984).

[34] J. G. Learned and S. Pakvasa, Astropart. Phys. **3**, 267 (1995).

[35] H. Athar, M. Jezabek, and O. Yasuda, Phys. Rev. D **62**, 103007 (2000); L. Bento, P. Keranen, and J. Maalampi, Phys. Lett. B **476**, 205 (2000).

[36] See also K. C. Lai, G. L. Lin, and T. C. Liu, Phys. Rev. D **82**, 103003 (2010).

[37] K. Abe *et al.* (T2K Collaboration), Phys. Rev. Lett. **107**, 041801 (2011).

[38] H. D. Kerret and the Double Chooz Collaboration, *LowNu11 Seoul* (National University, Seoul, 2011), p. 9.

[39] T. K. Gaisser, Astropart. Phys. **16**, 285 (2002).

[40] F. F. Lee and G. L. Lin, Astropart. Phys. **25**, 64 (2006).

[41] P. Lipari, Astropart. Phys. **1**, 195 (1993).

[42] T. K. Gaisser and M. Honda, Annu. Rev. Nucl. Part. Sci. **52**, 153 (2002).

[43] M. Honda, T. Kajita, K. Kasahara, and S. Midorikawa, Phys. Rev. D **70**, 043008 (2004).

[44] M. Honda, T. Kajita, K. Kasahara, S. Midorikawa, and T. Sanuki, Phys. Rev. D **75**, 043006 (2007).

[45] R. Abbasi *et al.*, Astropart. Phys. **34**, 48 (2010).

[46] T. K. Gaisser, *Cosmic Rays and Particle Physics* (Cambridge University Press, Cambridge, 1992).

[47] P. Nason, S. Dawson, and R. K. Ellis, Nucl. Phys. **B327**, 49 (1989); **B335**, 260(E) (1990); M. L. Mangano, P. Nason, and G. Ridolfi, Nucl. Phys. **B373**, 295 (1992).

[48] M. C. Gonzalez-Garcia, M. Maltoni, and J. Salvado, J. High Energy Phys. 04 (2010) 056.

[49] R. Gandhi, C. Quigg, M. H. Reno, and I. Sarcevic, Astropart. Phys. **5**, 81 (1996); Phys. Rev. D **58**, 093009 (1998).

[50] A. Abramowski *et al.* (H. E. S. S. Collaboration), Phys. Rev. Lett. **106**, 161301 (2011).

[51] J. Hisano *et al.*, Phys. Rev. D **83**, 123511 (2011).